HHS Public Access

Author manuscript

Cell Rep. Author manuscript; available in PMC 2016 May 05.

Published in final edited form as:

Cell Rep. 2015 May 5; 11(5): 785–797. doi:10.1016/j.celrep.2015.03.069.

DNA damage-induced type I interferon promotes senescence and inhibits stem cell function

Qiujing Yu[#1], **Yuliya V. Katlinskaya**[#1], **Christopher J. Carbone**[1], **Bin Zhao**[1], **Kanstantsin V. Katlinski**[1], **Hui Zheng**[1], **Manti Guha**[1], **Ning Li**[1], **Qijun Chen**[2], **Ting Yang**[2], **Christopher J. Lengner**[1], **Roger A. Greenberg**[2,3], **F. Brad Johnson**[2], and **Serge Y. Fuchs**[1,@]

[1]Department of Animal Biology, School of Veterinary Medicine, Abramson Family Cancer Research Institute, Basser Research Center for BRCA, Perelman School of Medicine, University of Pennsylvania, 380 S. University Ave, Philadelphia, PA 19104, USA

[2]Department of Pathology and Laboratory Medicine, Abramson Family Cancer Research Institute, Basser Research Center for BRCA, Perelman School of Medicine, University of Pennsylvania, 380 S. University Ave, Philadelphia, PA 19104, USA

[3]Department of Cancer Biology, Abramson Family Cancer Research Institute, Basser Research Center for BRCA, Perelman School of Medicine, University of Pennsylvania, 380 S. University Ave, Philadelphia, PA 19104, USA

[#] These authors contributed equally to this work.

Abstract

Expression of type I interferons (IFN) can be induced by DNA damaging agents but the mechanisms and significance of this regulation are not completely understood. We found that the transcription factor IRF3, activated in an ATM-IKKα/β dependent manner, stimulates cell-autonomous IFNβ expression in response to double-stranded DNA breaks. Cells and tissues with accumulating DNA damage produce endogenous IFNβ and stimulate IFN signaling *in vitro* and *in vivo*. In turn, IFN acts to amplify DNA damage responses, activate the p53 pathway, promote senescence and inhibit stem cells function in response to telomere shortening. Inactivation of the IFN pathway abrogates the development of diverse progeric phenotypes and extends the life span of *Terc* knockout mice. These data identify DNA damage response-induced IFN signaling as a critical mechanism that links accumulating DNA damage with senescence and premature aging.

[@]Corresponding author: Serge Y. Fuchs, syfuchs@vet.upenn.edu, tel. (215) 573-6949 fax (215) 746-2295 .

Contributions

S.Y.F., Q.Y., Y.V.K., C.J.L., R.A.G and F.B.J. designed the research; Q.Y., Y.V.K., C.J.C., B.Z., K.V.K., H.Z., M.G., Q.C., T.Y., N.L., S.Y.F., C.J.L., R.A.G and F.B.J. performed the experiments and interpreted the data; S.Y.F., C.J.L., R.A.G and F.B.J. wrote the manuscript with the help of all authors.

Competing financial interests

The authors declare no competing financial interests.

Keywords

interferon; DNA damage; aging; senescence; stem cells

Introduction

A link between aging and DNA damage is illustrated by the accumulation of DNA alterations seen in ageing human and mouse cells, accelerated aging phenotypes (progerias) observed in patients with hereditary impairments in genome maintenance, and progressive failure of stem cell function and aging-reminiscent tissue abnormalities observed in mouse models of persistent DNA damage responses (DDR) (Garinis et al., 2008; Hastie et al., 1990; Jiang et al., 2008; Lieber and Karanjawala, 2004; Sahin and Depinho, 2010). For example, knockout of the telomerase RNA component *Terc* causes progressive telomere shortening that persistently activates DDR and leads to numerous abnormalities in stem cell function and accelerated aging (Lee et al., 1998; Rudolph et al., 1999). At the cellular level, DDR promotes a permanent cell cycle arrest (senescence) – a cellular phenotype closely associated with aging of multicellular tissues and organs (Campisi, 2013; Campisi and d'Adda di Fagagna, 2007).

While the links between DDR and cell senescence/aging have been established, the molecular basis of this association is not well understood. The contribution of secreted factors that paracrinely propagate senescence has been extensively documented (Coppe et al., 2008a; Coppe et al., 2010; Coppe et al., 2008b; Tchkonia et al., 2013). However, the specific role of individual cytokines within this secretome is a subject of continuous investigation. Here we focused on type I interferons (IFN), - anti-viral cytokines including IFNβ and IFNα, that are expressed in response to activation of pathogen-associated molecular patterns under regulation of the IRF3 and IRF7 transcription factors, respectively (Katze et al., 2002). These IFN interact with the IFNAR1/IFNAR2 receptor complex to activate JAK-STAT signaling and induce IFN-stimulated genes (including *Irf7*, *Isg15* and *Ifitm3*), whose products elicit anti-viral effects, and contribute to the development of immunopathology (Bhattacharya et al., 2014; Trinchieri, 2010).

Recent reports indeed link DDR with IFN signaling. IFN-stimulated gene expression signatures are found in cells and tissues exposed to anti-cancer drugs and ionizing radiation known to induce DNA damage (Moschella et al., 2013; Weichselbaum et al., 2008). These agents were shown to either activate IRF3 (Kim et al., 1999) or stimulate production of IFN (Brzostek-Racine et al., 2011). Anti-tumorigenic effects of ionizing radiation and chemotherapy are at least in part mediated by effects of IFN whose production in animal tissues may rely on diverse pathogen recognition receptors (Burnette et al., 2011; Deng et al., 2014; Sistigu et al., 2014). Activation of IFN signaling is described in syndromes characterized by defects in enzymes processing/eliminating cytoplasmic DNA (Barber, 2011b; Stetson et al., 2008). Furthermore, genotoxic drug-induced cellular senescence correlates with production of IFN and induction of IFN-stimulated genes (Fridman and Tainsky, 2008; Mboko et al., 2012; Novakova et al., 2010).

However, while IFN expression is induced by radiation/anti-cancer drugs, it is not known whether IFN is induced by the DNA damage signals *per se* or is instead induced indirectly by accompanying induction of reactive oxygen species, which are known to stimulate IFN expression (Eguchi et al., 2011). In addition, while many pathogen recognition receptors may be involved in production of IFN by the debris of terminally damaged cells, it is not clear whether IFN can be produced in the same cell that undergoes DNA damage. Moreover, the physiologic role of the IFN produced in response to DNA damage is not completely understood.

Here we report that DNA damage itself can stimulate the production of IFNβ. Experiments using single-cell-based analyses demonstrate that low levels of IFNβ are increased rapidly and cell-autonomously in live cells within a few hours of the induction of double strand breaks (DSBs). This IFNβ production and associated cell senescence are greatly increased in cells from progeria patients deficient in genome maintenance genes and from knockout mice lacking the corresponding genes. Neutralizing the secreted IFNβ or knocking out/down its receptor attenuates cell senescence *in vitro*. Accordingly, *Ifnar1* ablation in *Terc*-deficient mice inhibits cell senescence *in vivo*, rescues mice from stem cell decline and mitigates premature aging-related alterations in multiple tissues and organs. These data implicate DDR-induced IFN in cell senescence and inhibition of stem cell function associated with accelerated aging.

Results

DNA damage activates cell-autonomous induction of IFNβ

To avoid side effects of radiation/chemotherapeutics and focus solely on the role of DNA damage, we used the expression of the telomere-specific binding protein TRF1 fused to FokI nuclease (FLAG-TRF1-FokI) that can induce DSBs in telomeric chromatin (Tang et al., 2013). This protein (but not nuclease-deficient TRF1-FokI^{D450A} mutant) increased expression of endogenous IFNβ protein (Figures 1A-B and S1A) and IFN-stimulated reporter (*Irf7* promoter-controlled IRF7-mCherry, (Rand et al., 2012), Figures 1C and S1B). These results together with attenuation of IRF7-mCherry expression by anti-IFNβ neutralizing antibody or siRNA (Figure 1C) indicate that DSBs inflicted by FokI activity stimulate IFNβ production to induce IRF7 expression.

We also utilized a U2OS fibrosarcoma stable cell line that co-expresses Lac operator-based DSB reporter (U2OSr (Shanbhag et al., 2010)) with mCherry-LacI-FokI nuclease fused to a destabilization domain and modified estradiol receptor. The resulting chimeric nuclease, which becomes expressed in cells upon treatment with the small molecules Shield ligand and 4-hydroxytamoxifen, incudes the appearance of a single localized DSB signal (Tang et al., 2013). We observed the phospho-γH2AX signal (within 3-6h of treatment) and concurrent increase of IFNβ levels in these cells (Figure 1D-E and 2A). In addition, induction of DSB led to activating phosphorylation of STAT1 and increase in IRF7 levels (Figure 1F) further linking DDR with the induction of IFN signaling.

Subsequent genetic experiments revealed attenuated IFN signaling (Figure 1F) and IFNβ expression (Figure 2A) in U2OSr cells treated with siRNA against IRF3. Intriguingly,

instead ofthe massive IRF3 nuclear import often reported in the virus-infected cells (Lin et al., 1998), we observed limited nuclear entry and a focal pattern including some co-localization of IRF3 within the vicinity of DSB (Figure 2B-C). A similar pattern was seen in parental U2OS cells treated with ionizing radiation (Figure S1C). These results suggest that DSBs stimulate IRF3 focal nuclear localization and IRF3-dependent expression of IFNβ.

An inhibitor of DNA-dependent serine/threonine protein kinase (DNA-PK, known to stimulate IRF3 nuclear retention (Karpova et al., 2002)) did not alter DSB-induced nuclear IRF3 foci (Figure 2C-D). Furthermore, these foci were not affected by RNAi against either Rnf8/Rnf168 ubiquitin ligases (linking DSB recognition with repair (Al-Hakim et al., 2010)) or ATF2 (known to regulate *Ifnb* transcription (Whitley et al., 1994)) but disappeared in cells receiving RNAi against IRF3 itself (Figure S1D). Importantly, treatment of cells with inhibitor of *Ataxia telangiectasia mutated* kinase ATM eliminated the phospho-H2AX foci and IRF3-positive foci (Figure 2C-D) as well as the elevated expression of IFNβ (Figure S1E) suggesting that ATM plays an important role in DDR signaling towards IRF3 activation and IFNβ production. While nuclear IRF3 foci persisted in cells transfected with siRNA against many known IRF3 regulators (such as STING, TBK1, RIG-I, MDA5, and IKKε (Hacker and Karin, 2006; Seth et al., 2006; Unterholzner, 2013)), the knockdown of IKKα or IKKβ IκB kinase species abrogated this IRF3 localization without affecting phospho-H2AX foci (Figure 2E). Either inhibition of ATM (but not DNA-PK) or knockdown of IKKα/IKKβ also noticeably decreased the induction of IFNβ in these cells (Figures 2A, S1E) suggesting that DSB-activated ATM can signal through IKKα/β to stimulate IRF3-driven IFNβ expression.

Notably, induction of DSB in U2OSr cells significantly increased the steady state *Ifnb* mRNA levels (Figure 3A). Transfection of double stranded DNA into mammalian cells has been previously shown to stimulate *Ifnb* expression (Li et al., 2005; Shirota et al., 2006). Intriguingly, when mouse genomic DNA was sonicated to induce DSBs, transfected cells that received the damaged DNA responded with a greater induction of *Ifnb* mRNA that did cells transfected with intact DNA. Remarkably, this DSB-induced *Ifnb* expression was sensitive to the ATM inhibitor (Figure 3B) further linking DDR with IFNβ production.

We then used human and mouse cells and tissues previously shown to accumulate DSBs (Du et al., 2004). Noticeably greater levels of *Ifnb* were seen in human diploid fibroblasts from patients with Werner or Hutchinson-Gilford progeria syndromes than from normal human fibroblasts (Figure 3C). Higher *Ifnb* expression was also seen in MRC-5 fibroblasts serially cultured to late passages (shown to accumulate DNA damage (Lawless et al., 2010)) compared to the early passage (Figure 3C). Furthermore, embryo fibroblasts from mice lacking *Terc* alone or in combination with the mutations in the Werner and Bloom 3′-5′ DNA helicases (Du et al., 2004) expressed greater *Ifnb* levels than wild type cells (Figure 3D). In addition, tissues from *Terc* knockout mice bred to shorten the telomeres and produce persistent DDR (Choudhury et al., 2007; Du et al., 2004; Ju et al., 2007) displayed substantially greater mRNA levels of *Ifnb* (but not *Ifna4*, (Figure 3E) and diverse IFN-stimulated genes (Figures 3F). Collectively, these results suggest that persistent DDR induces IFNβ and a functional IFN response *in vitro* and *in vivo*.

DDR-induced IFNβ promotes cell senescence

Cells exposed to chronic DDR secrete inflammatory cytokines that can permanently halt their division (Coppe et al., 2010; Tchkonia et al., 2013). Therefore, we sought to determine whether DDR-induced IFNβ has a role in promoting growth arrest and senescence. Treatment of fibroblasts from Werner and Hutchinson-Gilford progeria syndrome patients with neutralizing antibody against human IFNβ stimulated entrance of cells into S and G2M cell cycle phases (Figure 4A). Furthermore, an elevated level of senescence-associated β-galactosidase (SA-βGal)-positive cells (compared to normal IMR90 cells, Figure S2A) observed in cultures of patients' cells was also markedly reduced by anti-IFNβ antibody (Figure 4B). Similarly, this antibody treatment or knockdown of IFNAR1 decreased the number of SA-βGal-positive cells in late passage cultures of MRC5 fibroblasts (Figure S2B). Expression of other senescence markers such as macroH2A, heterochromatin protein-1β, $p21^{CIP1/WAF1}$ and $p16^{INK4A}$ was also attenuated by neutralizing IFNβ in human cells (Figure 4C).

Consistent with our previous report (Du et al., 2004), greater numbers of SA-βGal-positive cells were observed in *Terc*$^{-/-}$ and Werner-Bloom-Terc$^{-/-}$ embryo fibroblasts compared to cells from wild type mice (Figure S2C). Anti-IFNβ antibody treatment decreased senescence as judged by SA-βGal staining (Figure 4D) and expression of other senescence markers (Figure 4E). Furthermore cells from *Ifnar1*$^{-/-}$ mice cultured at normoxic conditions to stimulate oxidative stress-induced senescence exhibited significantly fewer senescent cells compared to wild type cells (Figure S2D). Together these data suggest that DDR-induced IFNβ mediates cell growth arrest and senescence.

IFN contributes to stem cell decline and premature aging

Telomere shortening and persistent DDR in the inbred *Terc*$^{-/-}$ mice lead to a decline in stem cell function in highly proliferative tissues resulting in phenotypic manifestations reminiscent of accelerated aging (Rudolph et al., 1999). Given that expression of IFNβ and IFN-stimulated genes was also elevated in these mice (Figure 3E-F) we sought to determine the role of IFN signaling in these phenotypes. To this end, we crossed G1 *Terc*$^{-/-}$ mice with animals lacking *Ifnar1* and bred them to G4 (Figure S3A). Though parental *Ifnar1*-deficient mice exhibited a trend for greater telomere lengths; concurrent *Terc* ablation dramatically shortened telomeres regardless of *Ifnar1* status. Accordingly, a similar extent of telomere shortening was found in G4 *Terc*$^{-/-}$*; Ifnar1*$^{+/+}$ ("SK") and G4 *Terc*$^{-/-}$*; Ifnar1*$^{-/-}$ ("DK") mice (Figure S3B). Although, our qPCR technique is more indicative of telomere abundance than telomere length, it would be surprising for the *Ifnar1* status to influence one without the other (for example, stimulate formation of extra-chromosomal telomere repeat entities, which we were unable to observe, see Figure 6A below). Thus, comparable telomere abundance between SK and DK mice let us directly compare the phenotypes in different tissues derived from these animals.

Whereas guts from young SK mice hardly displayed gross abnormalities (Figure S3C), such changes became evident at eight months of age. We found numerous distortions in the crypt and villus architecture in SK animals (Figure 5A), including crypt dropout (reduced crypt numbers in a given length of intestine), villus blunting and atrophy. In addition, prominent

lymphocytic infiltrates in the underlying stroma and thickening of the lamina propria were indicative of inflammatory process. Concurrent knockout of *Ifnar1* in age-matched DK mice restored normal crypt-and villus architecture, increased villus height and crypt numbers, and reduced inflammation (Figure 5A). These results suggest that IFN may play a role in the intestinal pathology caused by *Terc* deficiency.

Even at a young age we found evidence for increased IFN signaling in the gut of *Terc* knockout animals. Consistent with the observed ability of the DDR to induce IFN and IFN-stimulated genes *in vitro* (Figures 1, 3-4), intestinal tissues from 20-25 day old SK mice displayed elevated IRF7 levels (Figure 5B). Remarkably, a dramatic increase in senescence evident from SA-βGal-positive staining (Figure 5C-D) and decreased Ki67 staining (Figure 5E-F) was observed in SK but not in DK animals. Furthermore, a significantly reduced level of the cleaved caspase-3 was seen in DK mice compared to SK mice (Figure 5G-H). Collectively, these results suggest that proliferative arrest and increased apoptosis observed in late generation *Terc*-deficient mice depend on IFN signaling.

We next sought to identify the effectors of IFN signaling that mediate increased senescence and apoptosis. Prolonged treatment of cells with recombinant IFN was shown to induce DNA damage and p53 *in vitro* (Moiseeva et al., 2006; Takaoka et al., 2003). While the levels of telomere dysfunction-induced foci (TIFs) that reflect accumulation of 53BP1 on uncapped telomeres (Suram et al., 2012; Takai et al., 2003) were comparable in intestinal cells from SK and DK mice, TIFs were much less abundant than the non-telomere associated 53BP1 foci (Figure 6A). Furthermore, high non-telomere associated and overall levels of 53BP foci in intestinal tissues from young or old SK animals were decreased dramatically in the DK tissues (Figures 6A and S4A-B). These results suggest that endogenous IFN acts to amplify DDR signaling downstream of telomere end uncapping in $Terc^{-/-}$ mice. In addition, the robust increase in p53 staining in the intestines of *Terc*-deficient mice was attenuated by ablation of *Ifnar1* (Figure 6B). These *in vivo* results were also seen in tissue from eight month old mice (Figure S4C) and are consistent with the earlier observation that neutralization of endogenous IFNβ produced by DDR-exposed cells markedly reduced p53 levels (Figure 4C, E). Finally, *Ifnar1* ablation also mitigated the *Terc*-deficiency-induced increase in the cyclin-dependent kinase inhibitors $p16^{INK4a}$ (*Cdkn2a*) and $p21^{CIP1/WAF1}$ (*Cdkna1*) and apoptosis regulators Puma (*Bbc3*) and Bax (Figure 6C-D). These results are consistent with an important *in vivo* role of endogenous IFN in amplification of DDR signaling and activation of molecular regulators of senescence and apoptosis prompted by the telomere shortening.

Because inability to maintain telomere length leads to the failure of stem cells, we investigated the expression of the Wnt pathway-induced genes known to play an important role in intestinal stem cell self-renewal (Formeister et al., 2009). Intriguingly, expression of *Lgr5* and *Sox9* was noticeably increased in the $Ifnar1^{-/-}$ mice (Figure 6D) suggesting a role for IFN in the regulation of these Wnt targets. Importantly, knockout of *Ifnar1* relieved the inhibition of *Lgr5* and *Sox9* expression observed in $Terc^{-/-}$ intestines (Figure 6D). These data suggest that DDR-induced IFN may inhibit additional pathways that are essential for the function of intestinal stem cells.

We further compared the hematopoietic stem cell compartments in DK and SK mice. Consistent with the ability of IFN to stimulate LSK proliferation (Essers et al., 2009), relatively low number of hematopoietic Lineage$^-$ Sca1$^+$ c-Kit$^+$ stem/progenitor cells (LSK) was seen in *Ifnar1*-deficient bone marrow (Figure 7A). SK mice had low number of LSK cells and long-term self-renewing LSK CD150$^+$CD48$^-$ stem cells (Figures 7A-B), and SK bone marrow cells displayed a limited ability to form colonies *in vitro* (Figure 7C). Remarkably, both counts were increased by knockout of *Ifnar1* in the DK mice. These results point to the contribution of DDR-induced IFN to the depletion of hematopoietic stem cells and early progenitors in *Terc*$^{-/-}$ deficient animals (Figure 7A-B) and suggest that at least a part of this contribution (noticed in the *in vitro* assay) is cell autonomous and is not influenced by status of IFN signaling in the stem cell niche (Figure 7C). Furthermore, consistent with increased myeloid proliferation and lymphoid lineage failure in these mice (Ju et al., 2007) we found a greater number of myeloid cells and fewer lymphocytes in their spleens. Both phenotypes were reversed in DK mice (Figure S5A). In all, these data are suggestive of an important role for DDR-induced IFN in renewal/proliferation of hematopoietic stem cell and progenitors and their ability to contribute to a specific lineage.

We next sought to determine the role of IFN signaling in the germinal stem cell failure and fertility/fecundity problems reported in later generations of *Terc*-deficient mice (Lee et al., 1998; Rudolph et al., 1999). Depletion of germ cells and atrophy of seminiferous tubules observed in testes from *Terc*$^{-/-}$ mice were not seen in age matched DK mice (Figure 7D). Furthermore, *Ifnar1* ablation efficiently rescued a reduction in number of litters (Figure 7E) and litter size (Figure 7F) indicating that germinal stem cell failure triggered by persistent DDR signaling is mediated by IFN.

Terc-deficient mice exhibit other gross signs of premature aging, including frequent appearance of gray hair and overall body size reduction (Lee et al., 1998; Rudolph et al., 1999). We have also observed these phenotypes in the SK animals. Most remarkably, knockout of *Ifnar1* in these mice decreased the amount of gray hair and robustly increased animal body weight and size (Figures 7G and S5B). Finally, abrogation of IFN signaling substantially increased the longevity of *Terc*-deficient animals (Figure 7H). These results suggest that IFN signaling plays a central role in DDR-stimulated development of progeroid phenotypes arising from critically shortened telomeres.

Discussion

Here we demonstrate that DNA damage in mammalian cells can signal cell-autonomously to induce endogenous IFNβ in an ATM-IKKα/IKKβ-IRF3-dependent manner (Figures 1-3). Expression of endogenous IFNβ and IFN-stimulated genes is increased *in vitro* and *in vivo* in cells and tissues characterized by persistent DNA damage (Figure 3). This IFNβ further activates the p53-p21 axis and increases the levels of p16^{INK4} concurrent with robustly promoting cell senescence *in vitro* (Figure 4). Moreover, persistent DDR signaling and the resultant pathogenic sequelae observed in *Terc* knockout mice are alleviated by concomitant deficiency in *Ifnar1* signaling, which is responsible for induction of mediators of senescence and apoptosis (Figures 5-6), failure of stem cells and ensuing premature aging and shortened life span (Figure 7). Together these results demonstrate that DDR-induced IFN signaling

represents a key mechanism linking accumulation of DNA damage with cell senescence, stem cells failure, tissue aging, and premature death.

Current results including correlation between number of DSBs in foreign DNA and its ability to induce IFNβ (Figure 3B) demonstrate that DNA damage *per se* leads to cell-autonomous production of IFNβ. It is plausible that this phenomenon evolved to respond to DSB signals elicited by un-integrated viruses to limit virus-induced genomic DNA alterations (Katze et al., 2002) thereby guarding the genome integrity. The nature of a sensor for DSB that triggers signaling towards IFN production may plausibly differ from the known sensors/mediators of responses to un-damaged cytoplasmic dsDNA such as STING or AIMII (Barber, 2011a). The details of signaling leading to IRF3 activation via IKKα and IKKβ (previously shown to be activated by DNA damage in an ATM-dependent manner (McCool and Miyamoto, 2012)) remain to be elucidated. Roles of additional DNA damage-inducible regulators of *Ifnb* expression (e.g. NF-κB/AP1/ATF2 (Bhoumik et al., 2005; Herrlich et al., 1994; Lau et al., 2012)) and additional pathogen recognition receptor-mediated mechanisms are currently being investigated.

It has been suggested that the primary function of cell senescence is anti-viral defense (Reddel, 2010). Consistent with this hypothesis, our current data indicate that DDR-induced endogenous IFNβ, a major anti-viral cytokine, plays an important role in development of senescence (Figures 4-5). The mechanisms by which DDR-induced IFNβ contributes to cell senescence are likely to be complex. Current data suggest that IFNβ-stimulated activation of IFNAR1 and downstream IFN-stimulated genes (Figures 5, S2) that act in concert to promote the DNA damage-induced senescence. Underlying IFN-stimulated mechanisms may include amplification of the DDR (Figure 6A) and activation of the p53 pathway which functions as a central regulator of senescence (Ventura et al., 2007; Xue et al., 2007). Indeed, IFN mediates DDR-induced upregulation of p53, $p21^{CIP1/WAF1}$ and $p16^{INK4A}$, Figure 6), thereby identifying these proteins as important effectors of IFN signaling that links DNA damage and senescence. Additional roles of other IFN-inducible genes (e.g. *Ifi16/Aim2* (Duan et al., 2011)) that can contribute to development of cell senescence should not be ruled out.

Genetic ablation of *Ifnar1* abolishes pathological abnormalities *in vivo* associated with premature aging and death in animals where DDR persists due to telomere shortening (Figure 7). While our data demonstrate comparable levels of telomere dysfunction-induced foci in SK and DK cells, it is still plausible that IFN may have an auxiliary role in regulating telomere end capping/de-capping. However, the dramatic increase of non-telomere associated DNA damage in SK but not DK cells (Figure 6A) suggest that IFN amplifies DNA damage downstream of telomere deficiency. Regardless of the mechanisms contributing to the IFN-dependent pathology, the attenuation of *Terc*-deficient phenotypes by ablating *Ifnar1* is striking. Given that similar rescue was seen in p53 or $p21^{CIP1/WAF1}$ knockout mice (Chin et al., 1999; Choudhury et al., 2007) and the role of IFN in expression of these mediators (Figure 6), it is likely that the p53-p21 pathway functions as an effector of DDR-induced IFN signaling responsible for cellular senescence, failure of stem cell function and phenotypes associated with premature aging. Additional IFN-dependent

activation of $p16^{INK4A}$ and effect on some of Wnt pathway target genes (Figure 6) may also contribute to these processes.

As DNA damage accumulates with age and correlates with an age-related decline in stem cell function (Campisi and d'Adda di Fagagna, 2007), it is likely that IFN-mediated suppression of self-renewal capacity, exhaustive proliferation and ensuing senescence of stem cells may play an important role in aging of rapidly renewable tissues such as bone marrow and intestine. Our current data together with the demonstrated ability of IFN to stimulated proliferation of hematopoietic stem cells leading to their eventual depletion (Essers et al., 2009; Sato et al., 2009) suggest that DDR-induced IFN may act through this mechanism. The cell-autonomous role of IFN signaling in declining function of these cells is further supported by our *in vitro* data (Figure 7C). In addition, IFN might also act indirectly via altering the stem cell niche (demonstrated in *Terc* knockouts (Song et al., 2010)) and exacerbating inflammation in peripheral tissues (Bhattacharya et al., 2014).

Importantly, our *in vitro* and animal data presented here are consistent with clinical observations of increased cell senescence found in patients with hepatitis C undergoing treatment with IFN (Jurk et al., 2014). Furthermore, elevated IFN activities found in aging human and mouse brains were implicated in aging-related cognitive decline (Baruch et al., 2014). Further investigation of the role of IFN in accelerated and normal aging is warranted.

Methods

Animals

All experiments using animals were carried out under the protocols 803995 and 804470 approved by the IACUC of The University of Pennsylvania. All mice were of C57Bl/6J background and had water *ad libitum* and were fed regular chow. $Ifnar1^{-/-}$ mice (gift of Dr. Dong-Er Zhang, UCSD) were crossed with telomerase knockout mice (G1 $Terc^{-/-}$ (Blasco et al., 1997; Rudolph et al., 1999)) to generate $Terc^{+/-}$, $Ifnar1^{+/-}$ mice. These mice were backcrossed with $Ifnar1^{-/-}$ or $Ifnar1^{+/+}$ mice and then subjected to cousin mating through successive generations to produce G4 $Terc^{-/-}$, $Ifnar1^{-/-}$ (DK) or G4 $Terc^{-/-}$, $Ifnar1^{+/+}$ (SK) mice (Figure S3). Telomere length in genomic DNA from age-matched animals was assessed by quantitative PCR as reported elsewhere (Choudhury et al., 2007; Du et al., 2004; Ju et al., 2007). cDNA was used for quantitative PCR (with primers listed in Table S1) that was carried out using Applied Biosystems 7500 Fast Real-Time PCR system.

Cells

HeLa, 293T, IMR 90, NIH3T3 cells that stably express IRF7-mCherry fusion protein under control of *Irf7* promoter (Rand et al., 2012), U2OS and U2OS-reporter cells (U2OSr, described in details in (Tang et al., 2013)), primary mouse embryo fibroblasts from late generations $Terc^{-/-}$ mice (C57Bl/6J background) and $Wrn^{-/-}$ $Blm^{m3/m3}$ $Terc^{-/-}$ mice (mixed background: 50% C57BL/6J, 37.5% 129Svj, 12.5% BALB/c; described in (Du et al., 2004)) and MRC5 cells were cultured in DMEM plus 15% FBS. Human diploid fibroblast (HDF) cells from patients with Hutchinson-Gilford progeria syndrome (HGPS, cell line AG0989B) and Werner syndrome (WS, cell line AG05229B) were purchased from Coriell

Institute for Medical Research. MRC5, HGPS and WS cells were cultured in a Billups-Rothenberg modular incubator chambers at 3% O_2 until they were transferred to 20% O_2 culture condition to induce senescence. Transient transfections of cells with siRNA oligos (listed in Table S2) using Lipofectamine® RNAiMAX Transfection Reagent (Invitrogen).

qPCR, immunotechniques, etc

Immunoblotting and FACS analyses procedures were described previously (Bhattacharya et al., 2014; Li et al., 2004; Zheng et al., 2011). Analyses of dysfunctional telomere-induced foci were carried out in the intestines from *Terc*-deficient mice differing in the *Ifnar1* background. Tissue sections were hybridized with a Cy3-labeled PNA telomere repeat probe ((CCCTAA)3) and Alexa Fluor 488-labeled anti-53BP1 antibodies (Novus, NB100-304) as described in (Suram et al., 2012). Total 53BP1-positive foci per basal crypt were counted in 40 random fields. The number of positive cells per crypt (SA-βGal, Ki67) or per field (IRF7, cleaved caspase-3, and $p16^{INK4a}$) was counted in 20 random low-power fields. Each analysis was repeated in 3 mice per genotype group. Summary data are shown as mean ± S.E.M.

Supplementary Material

Refer to Web version on PubMed Central for supplementary material.

Acknowledgments

We thank M.M. Chou, J.R. Pehrson, D.E. Zhang and U. Rand for reagents, N.G. Avadhani, Z.A. Ronai, E. Lau and the members of Fuchs, Diehl, Koumenis, Greenberg, Witze and Minn labs (at the University of Pennsylvania) for critical suggestions, and L.B. King and A. Ortiz for help with manuscript preparation. This work was supported by NIH/NCI grants CA092900 and CA142425 (to SYF) and NIH P30-DK050306 (Molecular Pathology/Imaging Core, Molecular Biology Core).

References

Al-Hakim A, Escribano-Diaz C, Landry MC, O'Donnell L, Panier S, Szilard RK, Durocher D. The ubiquitous role of ubiquitin in the DNA damage response. DNA Repair (Amst). 2010; 9:1229–1240. [PubMed: 21056014]

Barber GN. Cytoplasmic DNA innate immune pathways. Immunol Rev. 2011a; 243:99–108. [PubMed: 21884170]

Barber GN. Innate immune DNA sensing pathways: STING, AIMII and the regulation of interferon production and inflammatory responses. Curr Opin Immunol. 2011b; 23:10–20. [PubMed: 21239155]

Baruch K, Deczkowska A, David E, Castellano JM, Miller O, Kertser A, Berkutzki T, Barnett-Itzhaki Z, Bezalel D, Wyss-Coray T, et al. Aging. Aging-induced type I interferon response at the choroid plexus negatively affects brain function. Science. 2014; 346:89–93. [PubMed: 25147279]

Bhattacharya S, Katlinski KV, Reichert M, Takano S, Brice A, Zhao B, Yu Q, Zheng H, Carbone CJ, Katlinskaya YV, et al. Triggering ubiquitination of IFNAR1 protects tissues from inflammatory injury. EMBO Mol Med. 2014; 6:384–397. [PubMed: 24480543]

Bhoumik A, Takahashi S, Breitweiser W, Shiloh Y, Jones N, Ronai Z. ATM-dependent phosphorylation of ATF2 is required for the DNA damage response. Mol Cell. 2005; 18:577–587. [PubMed: 15916964]

Blasco MA, Lee HW, Hande MP, Samper E, Lansdorp PM, DePinho RA, Greider CW. Telomere shortening and tumor formation by mouse cells lacking telomerase RNA. Cell. 1997; 91:25–34. [PubMed: 9335332]

Brzostek-Racine S, Gordon C, Van Scoy S, Reich NC. The DNA damage response induces IFN. J Immunol. 2011; 187:5336–5345. [PubMed: 22013119]

Burnette BC, Liang H, Lee Y, Chlewicki L, Khodarev NN, Weichselbaum RR, Fu YX, Auh SL. The efficacy of radiotherapy relies upon induction of type i interferon-dependent innate and adaptive immunity. Cancer Res. 2011; 71:2488–2496. [PubMed: 21300764]

Campisi J. Aging, cellular senescence, and cancer. Annu Rev Physiol. 2013; 75:685–705. [PubMed: 23140366]

Campisi J, d'Adda di Fagagna F. Cellular senescence: when bad things happen to good cells. Nat Rev Mol Cell Biol. 2007; 8:729–740. [PubMed: 17667954]

Chin L, Artandi SE, Shen Q, Tam A, Lee SL, Gottlieb GJ, Greider CW, DePinho RA. p53 deficiency rescues the adverse effects of telomere loss and cooperates with telomere dysfunction to accelerate carcinogenesis. Cell. 1999; 97:527–538. [PubMed: 10338216]

Choudhury AR, Ju Z, Djojosubroto MW, Schienke A, Lechel A, Schaetzlein S, Jiang H, Stepczynska A, Wang C, Buer J, et al. Cdkn1a deletion improves stem cell function and lifespan of mice with dysfunctional telomeres without accelerating cancer formation. Nat Genet. 2007; 39:99–105. [PubMed: 17143283]

Coppe JP, Boysen M, Sun CH, Wong BJ, Kang MK, Park NH, Desprez PY, Campisi J, Krtolica A. A role for fibroblasts in mediating the effects of tobacco-induced epithelial cell growth and invasion. Mol Cancer Res. 2008a; 6:1085–1098. [PubMed: 18644973]

Coppe JP, Desprez PY, Krtolica A, Campisi J. The senescence-associated secretory phenotype: the dark side of tumor suppression. Annu Rev Pathol. 2010; 5:99–118. [PubMed: 20078217]

Coppe JP, Patil CK, Rodier F, Sun Y, Munoz DP, Goldstein J, Nelson PS, Desprez PY, Campisi J. Senescence-associated secretory phenotypes reveal cell-nonautonomous functions of oncogenic RAS and the p53 tumor suppressor. PLoS Biol. 2008b; 6:2853–2868. [PubMed: 19053174]

Deng L, Liang H, Xu M, Yang X, Burnette B, Arina A, Li XD, Mauceri H, Beckett M, Darga T, et al. STING-Dependent Cytosolic DNA Sensing Promotes Radiation-Induced Type I Interferon-Dependent Antitumor Immunity in Immunogenic Tumors. Immunity. 2014; 41:843–852. [PubMed: 25517616]

Du X, Shen J, Kugan N, Furth EE, Lombard DB, Cheung C, Pak S, Luo G, Pignolo RJ, DePinho RA, et al. Telomere shortening exposes functions for the mouse Werner and Bloom syndrome genes. Mol Cell Biol. 2004; 24:8437–8446. [PubMed: 15367665]

Duan X, Ponomareva L, Veeranki S, Panchanathan R, Dickerson E, Choubey D. Differential roles for the interferon-inducible IFI16 and AIM2 innate immune sensors for cytosolic DNA in cellular senescence of human fibroblasts. Mol Cancer Res. 2011; 9:589–602. [PubMed: 21471287]

Eguchi H, Fujiwara N, Sakiyama H, Yoshihara D, Suzuki K. Hydrogen peroxide enhances LPS-induced nitric oxide production via the expression of interferon beta in BV-2 microglial cells. Neurosci Lett. 2011; 494:29–33. [PubMed: 21354265]

Essers MA, Offner S, Blanco-Bose WE, Waibler Z, Kalinke U, Duchosal MA, Trumpp A. IFNalpha activates dormant haematopoietic stem cells in vivo. Nature. 2009; 458:904–908. [PubMed: 19212321]

Formeister EJ, Sionas AL, Lorance DK, Barkley CL, Lee GH, Magness ST. Distinct SOX9 levels differentially mark stem/progenitor populations and enteroendocrine cells of the small intestine epithelium. Am J Physiol Gastrointest Liver Physiol. 2009; 296:G1108–1118. [PubMed: 19228882]

Fridman AL, Tainsky MA. Critical pathways in cellular senescence and immortalization revealed by gene expression profiling. Oncogene. 2008; 27:5975–5987. [PubMed: 18711403]

Garinis GA, van der Horst GT, Vijg J, Hoeijmakers JH. DNA damage and ageing: new-age ideas for an age-old problem. Nat Cell Biol. 2008; 10:1241–1247. [PubMed: 18978832]

Hacker H, Karin M. Regulation and function of IKK and IKK-related kinases. Sci STKE. 2006; 2006:re13. [PubMed: 17047224]

Hastie ND, Dempster M, Dunlop MG, Thompson AM, Green DK, Allshire RC. Telomere reduction in human colorectal carcinoma and with ageing. Nature. 1990; 346:866–868. [PubMed: 2392154]

Herrlich P, Sachsenmaier C, Radler-Pohl A, Gebel S, Blattner C, Rahmsdorf HJ. The mammalian UV response: mechanism of DNA damage induced gene expression. Adv Enzyme Regul. 1994; 34:381–395. [PubMed: 7942283]

Jiang H, Schiffer E, Song Z, Wang J, Zurbig P, Thedieck K, Moes S, Bantel H, Saal N, Jantos J, et al. Proteins induced by telomere dysfunction and DNA damage represent biomarkers of human aging and disease. Proc Natl Acad Sci U S A. 2008; 105:11299–11304. [PubMed: 18695223]

Ju Z, Jiang H, Jaworski M, Rathinam C, Gompf A, Klein C, Trumpp A, Rudolph KL. Telomere dysfunction induces environmental alterations limiting hematopoietic stem cell function and engraftment. Nat Med. 2007; 13:742–747. [PubMed: 17486088]

Jurk D, Wilson C, Passos JF, Oakley F, Correia-Melo C, Greaves L, Saretzki G, Fox C, Lawless C, Anderson R, et al. Chronic inflammation induces telomere dysfunction and accelerates ageing in mice. Nat Commun. 2014; 2:4172. [PubMed: 24960204]

Karpova AY, Trost M, Murray JM, Cantley LC, Howley PM. Interferon regulatory factor-3 is an in vivo target of DNA-PK. Proc Natl Acad Sci U S A. 2002; 99:2818–2823. [PubMed: 11867762]

Katze MG, He Y, Gale M Jr. Viruses and interferon: a fight for supremacy. Nat Rev Immunol. 2002; 2:675–687. [PubMed: 12209136]

Kim T, Kim TY, Song YH, Min IM, Yim J, Kim TK. Activation of interferon regulatory factor 3 in response to DNA-damaging agents. J Biol Chem. 1999; 274:30686–30689. [PubMed: 10521456]

Lau E, Kluger H, Varsano T, Lee K, Scheffler I, Rimm DL, Ideker T, Ronai ZA. PKCepsilon promotes oncogenic functions of ATF2 in the nucleus while blocking its apoptotic function at mitochondria. Cell. 2012; 148:543–555. [PubMed: 22304920]

Lawless C, Wang C, Jurk D, Merz A, Zglinicki T, Passos JF. Quantitative assessment of markers for cell senescence. Exp Gerontol. 2010; 45:772–778. [PubMed: 20117203]

Lee HW, Blasco MA, Gottlieb GJ, Horner JW 2nd, Greider CW, DePinho RA. Essential role of mouse telomerase in highly proliferative organs. Nature. 1998; 392:569–574. [PubMed: 9560153]

Li S, Wilkinson M, Xia X, David M, Xu L, Purkel-Sutton A, Bhardwaj A. Induction of IFN-regulated factors and antitumoral surveillance by transfected placebo plasmid DNA. Mol Ther. 2005; 11:112–119. [PubMed: 15585412]

Li Y, Gazdoiu S, Pan ZQ, Fuchs SY. Stability of homologue of Slimb F-box protein is regulated by availability of its substrate. J Biol Chem. 2004; 279:11074–11080. [PubMed: 14707120]

Lieber MR, Karanjawala ZE. Ageing, repetitive genomes and DNA damage. Nat Rev Mol Cell Biol. 2004; 5:69–75. [PubMed: 14708011]

Lin R, Heylbroeck C, Pitha PM, Hiscott J. Virus-dependent phosphorylation of the IRF-3 transcription factor regulates nuclear translocation, transactivation potential, and proteasome-mediated degradation. Mol Cell Biol. 1998; 18:2986–2996. [PubMed: 9566918]

Mboko WP, Mounce BC, Wood BM, Kulinski JM, Corbett JA, Tarakanova VL. Coordinate regulation of DNA damage and type I interferon responses imposes an antiviral state that attenuates mouse gammaherpesvirus type 68 replication in primary macrophages. J Virol. 2012; 86:6899–6912. [PubMed: 22496235]

McCool KW, Miyamoto S. DNA damage-dependent NF-kappaB activation: NEMO turns nuclear signaling inside out. Immunol Rev. 2012; 246:311–326. [PubMed: 22435563]

Moiseeva O, Mallette FA, Mukhopadhyay UK, Moores A, Ferbeyre G. DNA damage signaling and p53-dependent senescence after prolonged beta-interferon stimulation. Mol Biol Cell. 2006; 17:1583–1592. [PubMed: 16436515]

Moschella F, Torelli GF, Valentini M, Urbani F, Buccione C, Petrucci MT, Natalino F, Belardelli F, Foa R, Proietti E. Cyclophosphamide induces a type I interferon-associated sterile inflammatory response signature in cancer patients' blood cells: implications for cancer chemoimmunotherapy. Clin Cancer Res. 2013; 19:4249–4261. [PubMed: 23759676]

Novakova Z, Hubackova S, Kosar M, Janderova-Rossmeislova L, Dobrovolna J, Vasicova P, Vancurova M, Horejsi Z, Hozak P, Bartek J, Hodny Z. Cytokine expression and signaling in drug-induced cellular senescence. Oncogene. 2010; 29:273–284. [PubMed: 19802007]

Rand U, Rinas M, Schwerk J, Nohren G, Linnes M, Kroger A, Flossdorf M, Kaly-Kullai K, Hauser H, Hofer T, Koster M. Multi-layered stochasticity and paracrine signal propagation shape the type-I interferon response. Mol Syst Biol. 2012; 8:584. [PubMed: 22617958]

Reddel RR. Senescence: an antiviral defense that is tumor suppressive? Carcinogenesis. 2010; 31:19–26. [PubMed: 19887513]

Rudolph KL, Chang S, Lee HW, Blasco M, Gottlieb GJ, Greider C, DePinho RA. Longevity, stress response, and cancer in aging telomerase-deficient mice. Cell. 1999; 96:701–712. [PubMed: 10089885]

Sahin E, Depinho RA. Linking functional decline of telomeres, mitochondria and stem cells during ageing. Nature. 2010; 464:520–528. [PubMed: 20336134]

Sato T, Onai N, Yoshihara H, Arai F, Suda T, Ohteki T. Interferon regulatory factor-2 protects quiescent hematopoietic stem cells from type I interferon-dependent exhaustion. Nat Med. 2009; 15:696–700. [PubMed: 19483695]

Seth RB, Sun L, Chen ZJ. Antiviral innate immunity pathways. Cell Res. 2006; 16:141–147. [PubMed: 16474426]

Shanbhag NM, Rafalska-Metcalf IU, Balane-Bolivar C, Janicki SM, Greenberg RA. ATM-dependent chromatin changes silence transcription in cis to DNA double-strand breaks. Cell. 2010; 141:970–981. [PubMed: 20550933]

Shirota H, Ishii KJ, Takakuwa H, Klinman DM. Contribution of interferon-beta to the immune activation induced by double-stranded DNA. Immunology. 2006; 118:302–310. [PubMed: 16827891]

Sistigu A, Yamazaki T, Vacchelli E, Chaba K, Enot DP, Adam J, Vitale I, Goubar A, Baracco EE, Remedios C, et al. Cancer cell-autonomous contribution of type I interferon signaling to the efficacy of chemotherapy. Nat Med. 2014; 20:1301–1309. [PubMed: 25344738]

Song Z, Wang J, Guachalla LM, Terszowski G, Rodewald HR, Ju Z, Rudolph KL. Alterations of the systemic environment are the primary cause of impaired B and T lymphopoiesis in telomere-dysfunctional mice. Blood. 2010; 115:1481–1489. [PubMed: 19965646]

Stetson DB, Ko JS, Heidmann T, Medzhitov R. Trex1 prevents cell-intrinsic initiation of autoimmunity. Cell. 2008; 134:587–598. [PubMed: 18724932]

Suram A, Kaplunov J, Patel PL, Ruan H, Cerutti A, Boccardi V, Fumagalli M, Di Micco R, Mirani N, Gurung RL, et al. Oncogene-induced telomere dysfunction enforces cellular senescence in human cancer precursor lesions. EMBO J. 2012; 31:2839–2851. [PubMed: 22569128]

Takai H, Smogorzewska A, de Lange T. DNA damage foci at dysfunctional telomeres. Curr Biol. 2003; 13:1549–1556. [PubMed: 12956959]

Takaoka A, Hayakawa S, Yanai H, Stoiber D, Negishi H, Kikuchi H, Sasaki S, Imai K, Shibue T, Honda K, Taniguchi T. Integration of interferon-alpha/beta signalling to p53 responses in tumour suppression and antiviral defence. Nature. 2003; 424:516–523. [PubMed: 12872134]

Tang J, Cho NW, Cui G, Manion EM, Shanbhag NM, Botuyan MV, Mer G, Greenberg RA. Acetylation limits 53BP1 association with damaged chromatin to promote homologous recombination. Nat Struct Mol Biol. 2013; 20:317–325. [PubMed: 23377543]

Tchkonia T, Zhu Y, van Deursen J, Campisi J, Kirkland JL. Cellular senescence and the senescent secretory phenotype: therapeutic opportunities. J Clin Invest. 2013; 123:966–972. [PubMed: 23454759]

Trinchieri G. Type I interferon: friend or foe? J Exp Med. 2010; 207:2053–2063. [PubMed: 20837696]

Unterholzner L. The interferon response to intracellular DNA: why so many receptors? Immunobiology. 2013; 218:1312–1321. [PubMed: 23962476]

Ventura A, Kirsch DG, McLaughlin ME, Tuveson DA, Grimm J, Lintault L, Newman J, Reczek EE, Weissleder R, Jacks T. Restoration of p53 function leads to tumour regression in vivo. Nature. 2007; 445:661–665. [PubMed: 17251932]

Weichselbaum RR, Ishwaran H, Yoon T, Nuyten DS, Baker SW, Khodarev N, Su AW, Shaikh AY, Roach P, Kreike B, et al. An interferon-related gene signature for DNA damage resistance is a predictive marker for chemotherapy and radiation for breast cancer. Proc Natl Acad Sci U S A. 2008; 105:18490–18495. [PubMed: 19001271]

Whitley MZ, Thanos D, Read MA, Maniatis T, Collins T. A striking similarity in the organization of the E-selectin and beta interferon gene promoters. Mol Cell Biol. 1994; 14:6464–6475. [PubMed: 7523851]

Xue W, Zender L, Miething C, Dickins RA, Hernando E, Krizhanovsky V, Cordon-Cardo C, Lowe SW. Senescence and tumour clearance is triggered by p53 restoration in murine liver carcinomas. Nature. 2007; 445:656–660. [PubMed: 17251933]

Zheng H, Qian J, Varghese B, Baker DP, Fuchs S. Ligand-stimulated downregulation of the alpha interferon receptor: role of protein kinase D2. Mol Cell Biol. 2011; 31:710–720. [PubMed: 21173164]

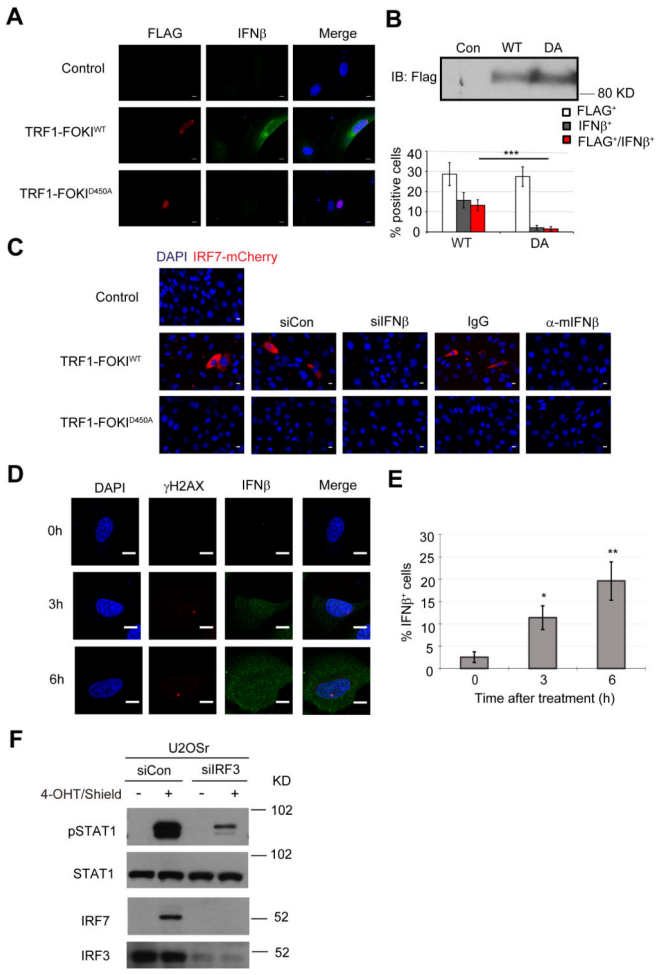

Figure 1.

Induction of double strand breaks leads to production of functional IFNβ protein

A. IFNβ protein was detected in FLAG-tagged TRF1-FokI (wild type or nuclease-inactive D450A mutant)-transfected mouse embryo fibroblasts. Immunofluorescence using indicated antibodies is shown. Magnification bar for all panels: 10 μm.

B. Levels of TRF-FokI proteins detected by immunoblotting (upper panel) and quantification of percent of cells single or double positive (red bars) for FLAG and IFNβ proteins in 22-25 fields randomly chosen from 3 independent experiments performed as described in A (lower panel). Here and thereafter: data are shown as average± S.E.M.; * $p<0.05$; ** $p<0.01$; ***$p<0.001$.

C. Expression of *Irf7* promoter-driven IRF7-mCherry fusion protein in TRF1-FokI-transfected NIH3T3 cells treated as indicated with RNAi (control or against *Ifnb*) or antibodies (control IgG or neutralizing antibody against mouse IFNβ, 10 μg/ml for 72h after transfection).

D. Immunofluorescent detection of IFNβ-positive cells after induction of DSB with 4-OHT (2.5μM) and Shield (1μM) compound for indicated times in the U2OS-DSB reporter cells (U2OSr) cells.

E. Quantification of data shown in D in 9-11 fields randomly chosen from 3 independent experiments.

F. Immunoblot analysis of lysates from the U2OSr cells transfected with indicated RNAi and treated or not with 4-OHT (2.5μM) and Shield (1μM) compound for 6h.

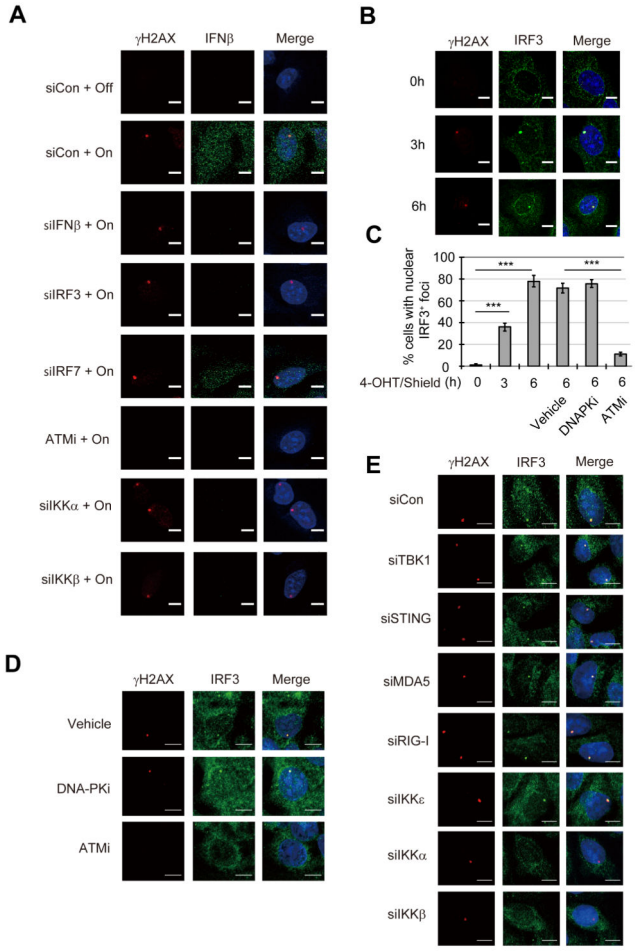

Figure 2.

Effect of DSB induction on IRF3 localization

A. Immunofluorescent detection of IFNβ-positive cells before (“off”) or after (“on”) induction of DSB with 4-OHT (2.5μM) and Shield (1μM) compound for 6h in the U2OSr cells that were prior either transfected with indicated siRNA oligos for 66h or pretreated with ATM inhibitor (Ku55933,10μM for 1h). Magnification bar for all panels: 10 μm.

B. Recruitment of IRF3 to the DNA damage foci after inducing DSB with 4-OHT/Shield compounds for indicated times detected by immunofluorescence in the U2OSr cells.

C. Quantification of cells containing IRF3-positive foci in the nucleus in 8-10 fields randomly chosen from 3 independent experiments performed as described in panels B and D.

D. Recruitment of IRF3 to the DNA damage foci in the U2OSr cells pre-treated with vehicle or ATM inhibitor (Ku55933, 10μM for 1h) or DNA-PK inhibitor (Nu7441, 4μM for 1h) as indicated.

E. IRF3 localization in U2OSr cells that received indicated siRNA oligos 66h before inducing DSB with 4-OHT (2.5μM) and Shield (1μM) compound as in panel D.

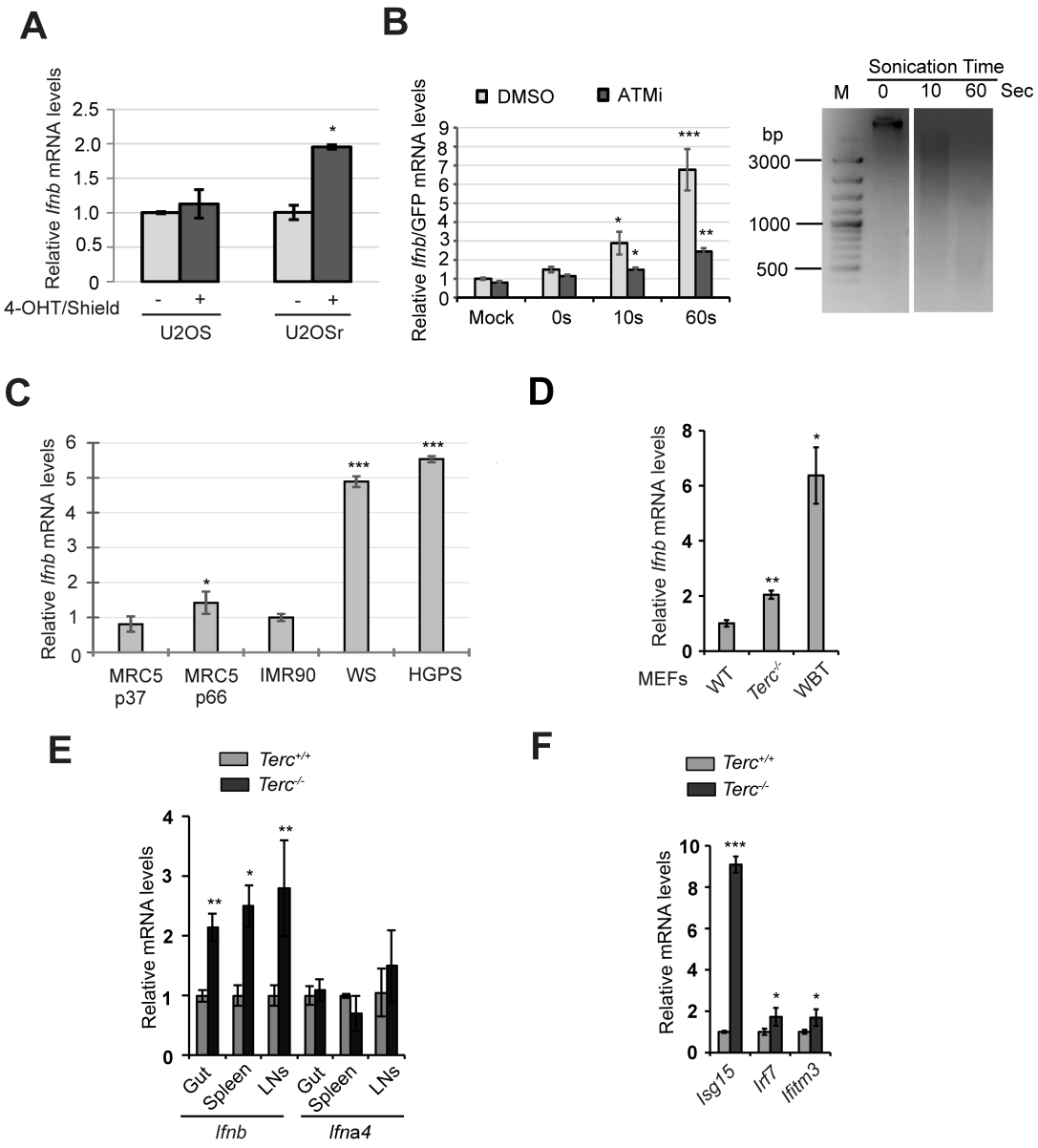

Figure 3.

DSB induces expression of mRNA of IFNβ

A. Relative expression of *Ifnb* mRNA in response to combined treatment with 4-OHT/Shield in parental U2OS cells and U2OSr cells.

B. Relative expression of *Ifnb* mRNA normalized per GFP mRNA levels in NIH3T3 cells co-transfected with mouse genomic DNA (1μg, sonicated for indicated times) and GFP plasmid (100ng) per 12-well plate well. Average data from 3 experiments (each in triplicate) are shown. The right panel depicts a representative ethidium bromide-stained agarose gel demonstrating the length of DNA fragments used for transfection. M (Markers): GeneRuler 100bp Plus DNA Ladder.

C. Relative levels of *Ifnb* mRNA in human fibroblasts (IMR90 levels taken as 1.0). Asterisks indicates significant differences between MRC5 fibroblasts cultured for 66

passages over those cultured for 37 passages (each passage being a two-fold split) and between fibroblasts from patients with Werner syndrome (WS, passage 23) or Hutchinson-Gilford Progeria Syndrome (HGPS, passage 23) and normal IMR90 (passage 25).

D. Relative levels of *Ifnb* mRNA in fibroblasts from wild type (WT, taken as 1.0), late generation $Terc^{-/-}$or Werner-Bloom-Terc deficient animals (WBT).

E. Relative levels of *Ifnb* and *Ifna4* mRNA in gut, spleen and lymph nodes (LNs) tissues from late generation $Terc^{-/-}$ mice compared to that in wild type mice (taken as 1.0).

F. Relative levels of indicated IFN-stimulated genes mRNA in spleen tissues from late generation $Terc^{-/-}$ mice compared to that in wild type mice (taken as 1.0).

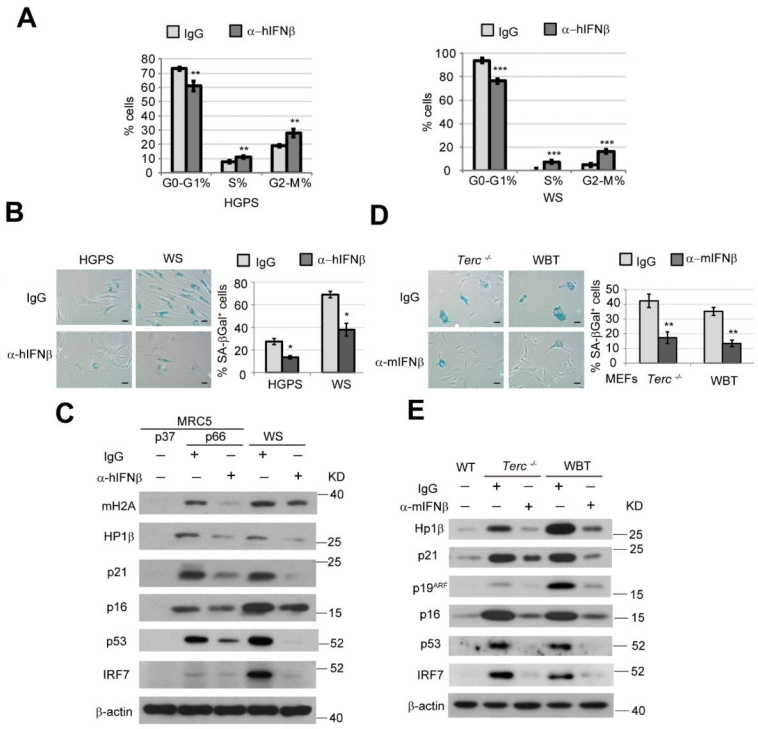

Figure 4.

Role of IFNβ in DNA-damage-induced senescence of mouse and human fibroblasts

A. Cell cycle distribution of fibroblasts from patients with Hutchinson Gilford Progeria (HGPS) and Werner (WS) syndrome cultured in the presence of neutralizing antibody against human IFNβ or control antibody (IgG, both at 10μg/mL for 48 hours).

B. Expression of SA-βGal by HGPS and WS human fibroblasts cultured in the presence of neutralizing antibody against human IFNβ or control antibody (IgG, both at 10μg/mL for 3-4 days). Magnification bar: 100 μm. Quantitated data reflect at least 200 total cells counted in 3 independent experiments.

C. Expression of protein markers of senescence (mH2A, Hp1β, p21, p16, p53) in MRC5 fibroblasts (passage 37 or 66) and in WS fibroblasts was analyzed by immunoblotting using the indicated antibodies. IRF7 protein levels serve as an IFN-induced gene product control. Levels of β-actin were used as a loading control.

D. Expression of SA-βGal by *Terc*$^{-/-}$ and WBT fibroblasts cultured in the presence of neutralizing antibody against murine IFNβ or control antibody (IgG, both at 10μg/mL for 10 days). Magnification bar: 100 μm. Quantitated data reflect at least 200 total cells counted in 3 independent experiments.

E. Expression of protein markers of senescence (Hp1β, p21, p16, p53 and p19^{ARF}) in wild type, *Terc*$^{-/-}$ and WBT fibroblasts was analyzed by immunoblotting using the indicated antibodies. IRF7 protein levels serve as an IFN-induced gene product control. Levels of β-actin were used as a loading control.

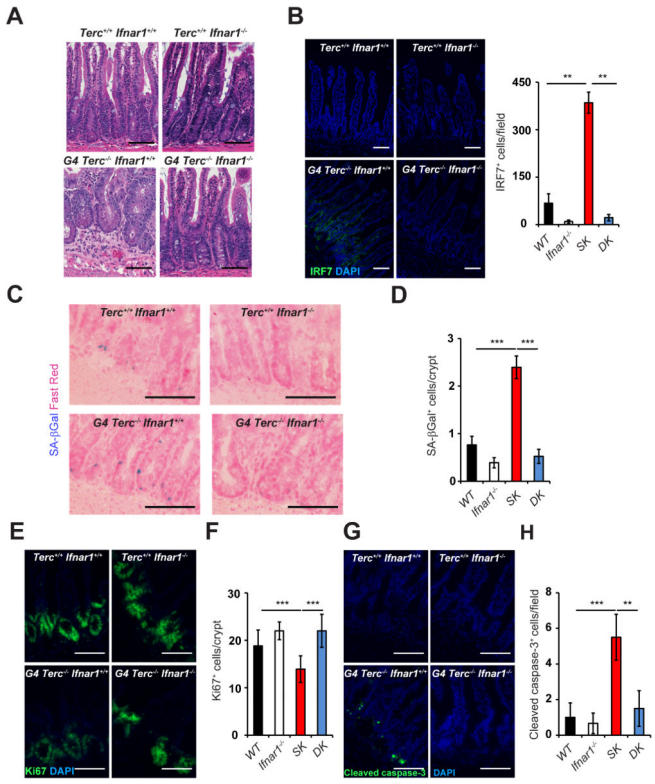

Figure 5.

IFN-dependent proliferative failure, senescence and apoptosis in the gut tissues from *Terc*-deficient mice is rescued by *Ifnar1* ablation

A. Hematoxylin and eosin (H&E) staining of the intestinal tissues from eight month old male mice of indicated genotypes. Magnification bar here and thereafter: 100μm.

B. Immunofluorescent analysis of IRF7 expression in the intestinal tissues of 22-25 day old mice of indicated genotypes. Right panel depicts the number of IRF7-positive cells per field in the small intestines of 3 mice (at least 10 random fields observed for each).

C. Analysis of SA-βgal positive cells in the intestinal tissues (counterstained with Nuclear Fast Red) of 22-25 day old mice of indicated genotypes.

D. Quantitation of the number of SA-βGal positive cells per basal crypt in the small intestines of 3 mice (30-100 crypts were analyzed for each).

E. Immunofluorescent analysis of Ki67 levels in the intestinal tissues of 22-25 day old mice of indicated genotypes.

F. Quantitation of the number of Ki67 positive cells per basal crypt in the small intestines of 3 mice (30-100 crypts were analyzed for each).

G. Immunofluorescent analysis of cleaved caspase-3 levels in the intestinal tissues of 22-25 day old mice of indicated genotypes.

H. Quantitation of the number of cleaved caspase-3 -positive cells per field in the small intestines (at least 10 random fields observed for each of 3 mice).

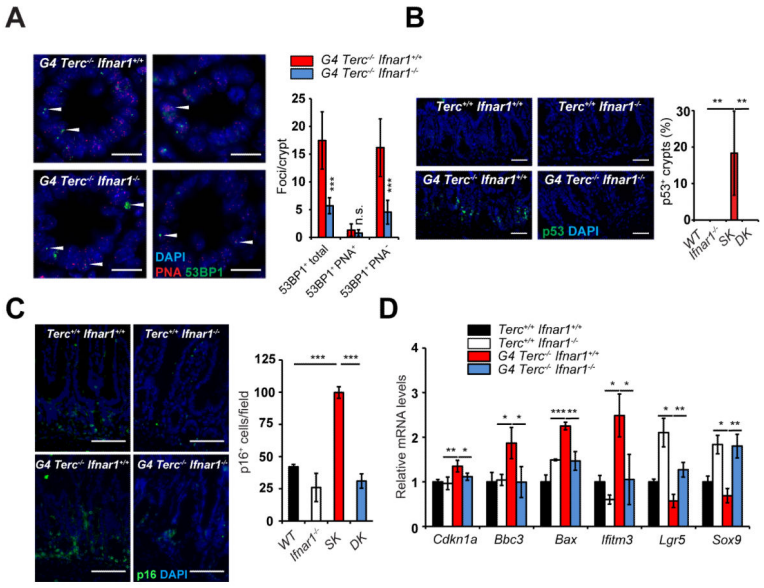

Figure 6.

IFN signaling amplifies DDR and ensuing expression of senescence mediators in the intestines from *Terc*-deficient mice

A. Immunofluorescent analysis of telomere dysfunction-induced foci (arrows) using PNA telomere probe and anti-53BP1 antibodies. Two representative crypts are shown for each *Ifnar1* background (top for SK, and bottom for DK). The number of PNA-associated, non-PNA-associated and total 53BP1 foci per intestinal crypt was scored in at least 50 crypts. Magnification bar: 20 μm.

B. Immunofluorescent analysis of p53 expression in the intestinal tissues from 22-25 day old mice of indicated genotypes. Right panel depicts the percentage of p53-positive crypts in the small intestines (30-100 crypts were analyzed for each of 3 mice). Magnification bar: 50 μm.

C. Immunofluorescent analysis of $p16^{INK4A}$ expression in the intestinal tissues from 22-25 day old mice of indicated genotypes. Right panel depicts the number of $p16^{INK4A}$-positive cells per field (at least 10 random fields observed for each of 3 mice). Magnification bar: 100 μm.

D. Relative mRNA levels of indicated genes in the indicated mouse intestines assessed by qPCR (levels in wild type mice taken as 1.0). Expression of *Ifit3m* mRNA was used as a control for a bona fide IFN-stimulated gene.

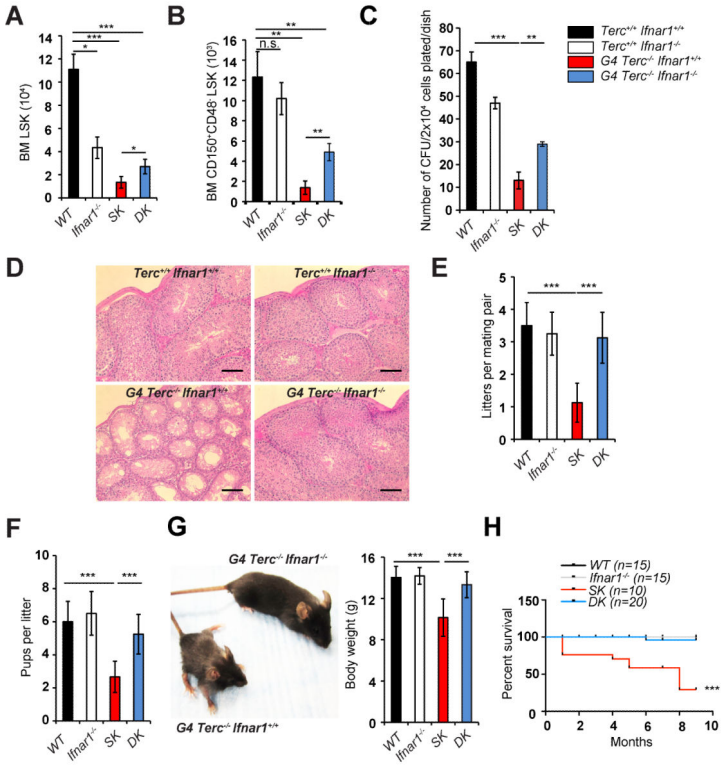

Figure 7.

DDR-induced IFN signals play a key role in failure of stem and germ cells and development of phenotypes associated with premature aging in the *Terc*-deficient mice

A. Number of hematopoietic precursor cells (LSK) in the bone marrow from 22-25 day old mice of indicated genotypes calculated from at least 4 individual animals.

B. Number of hematopoietic stem cells (LSK $CD150^{+}CD48^{-}$) in the bone marrow from 22-25 day old mice of indicated genotypes calculated from at least 4 individual animals.

C. Colony forming efficiency of bone marrow cells from age matched mice of indicated genotype.

D. H&E staining of the testis tissues from 22-25 day old male mice of indicated genotypes.

E. Number of litters per a mating pair (per first 4 months of mating) in mice of indicated genotypes (n=8 pairs for each genotype).

F. Number of pups per litter in in mice of indicated genotypes (n=7 for litters per each genotype)

G. Characteristic physical appearance and average body weight of 22-25 days old mice of indicated genotypes (n=10).

H. Kaplan-Meier analysis of survival of G4 mice of indicated genotypes.